Effect of ion implantation on surface energy of ultrahigh molecular weight polyethylene

J. S. Chen, Z. Sun, P. S. Guo, Z. B. Zhang, D. Z. Zhu et al.

Citation: J. Appl. Phys. **93**, 5103 (2003); doi: 10.1063/1.1559943
View online: http://dx.doi.org/10.1063/1.1559943
View Table of Contents: http://jap.aip.org/resource/1/JAPIAU/v93/i9
Published by the American Institute of Physics.

Effect of ion implantation on surface energy of ultrahigh molecular weight polyethylene

J. S. Chen, Z. Sun, and P. S. Guo[a)]
Nanotech Center, East China Normal University, Zhongshan N. Road 3663, Shanghai, 200062, People's Republic of China

Z. B. Zhang, D. Z. Zhu, and H. J. Xu
Shanghai Institute of Nuclear Research, Academia Sinica, P.O. Box 800-204, Shanghai, 201800, People's Republic of China

(Received 13 September 2002; accepted 20 January 2003)

The effect of ion implantation including ion species (N_2^+ and $C_3H_8^+$) and the fluences (1×10^{14}–5×10^{15} ions/cm^2) on the surface energy of ultrahigh molecular weight polyethylene (UHMWPE) were investigated. The total surface energy increases significantly after implanting with the fluence of 1×10^{14} ions/cm^2 regardless of ion species, then, the total surface energy slightly increases for N_2^+ implanted UHMWPE and decreases slightly for $C_3H_8^+$ implanted UHMWPE with a further increase of fluence. The structural changes of UHMWPE with different fluence for different ion species are very similar. The linear chains of UHMWPE are damaged and cross linking is generated after implantation. As the fluence increases, the polymer surface becomes more disordered, and the surface becomes hydrogenated amorphous carbon when the fluence exceeds 1×10^{15} ions/cm^2. The surface roughness increases with the increase of the fluence regardless of ion implantation species. © *2003 American Institute of Physics.* [DOI: 10.1063/1.1559943]

I. INTRODUCTION

Ion implantation is a technology which can produce metastable layers in materials via nonequilibrium processes.[1] In addition to providing a mechanism for introducing foreign species into a host materials, ion implantation can be employed to reproducibly and controllably alter the surface structure leading to desirable changes in the surface properties of the materials. Ion implantation technology has been successfully applied to the modification of metal, semiconductor, and ceramic as well as polymer for improving their surface properties such as the wear resistance, electrical resistance, and optical properties.[2–7] In recent years, ion implantation has also been used to modify polymers for improving their biocompatibility. These biomaterials usually require a hydrophilic surface for improving their biocompatibility e.g., the cell adhesion property.[8] Satisfactory results have been achieved by ion implantation in several polymer biomaterials like polystyrene, segmented polyurethane, and silicon rubber for improving wettability and biocompatibility of blood and adhesion property of bovine vascular endothelial cells.[9,10] In addition, surface interaction with tissue-enhancing moieties is thought to be mediated by increased wettability.[11] Wettability can be related to the surface energies of the solids and liquids involved.

Ultrahigh molecular weight polyethylene (UHMWPE) is generally used for a component of artificial joints which is against another component—a metallic articulating. The main problem in existing artificial joints is the prosthetic wear debris which is believed to the major reason for aseptic loosening.[12,13] The increase of wear resistance of UHMWPE has been achieved by ion implantation.[14–16] In the present work, we report the effect of ion implantation parameters such as ion fluence and ion species on the surface energy. Moreover, in order to further understand the mechanism of the change of surface energy, some other surface properties, such as structural and morphological properties and surface roughness, were investigated by micro-Raman spectroscopy, atomic force microscopy (AFM), and surface profiler.

II. EXPERIMENT

A. Sample preparation

UHMWPE used has an average molecular weight of 5 million g/mol and density of 0.937 g/cm^3. The UHMWPE samples were first polished mechanically, and then implanted by 80 keV N_2^+ and $C_3H_8^+$ with the fluence ranging from 1×10^{14} ions/cm^2 to 5×10^{15} ions/cm^2 by a Z-200 ion implantation machine. During implantation, the pressure of the chamber was 6.6×10^{-4} Pa. The beam current density was less than 0.1 mA/cm^2. The sample holder was cooled by flowing water and the temperature of the specimen was lower than 100 °C.

B. Surface energy analysis and contact angle measurement

The surface free energy (or surface tension) of the sample was determined by contact angle measurements. The first and probably most famous description of the correlations between the contact angle and surface free energy of a solid surface and liquid was provided by Young when a drop of liquid was on a solid surface.[17] And Young's equation is

a)Author to whom correspondence should be addressed; electronic mail: psguo@sh163.net

TABLE I. The dispersive ($\gamma_{\ell\nu}^{d}$) and polar ($\gamma_{\ell\nu}^{p}$) components and total surface energy ($\gamma_{\ell\nu}$) for selected test liquids.

Liquid	$\gamma_{\ell\nu}^{d}$ (dyne/cm)	$\gamma_{\ell\nu}^{p}$ (dyne/cm)	$\gamma_{\ell\nu}$ (dyne/cm)
Water	22.1	50.7	72.8
Formamide	39.5	18.7	58.2

$$\gamma_{s\nu}=\gamma_{s\ell}+\gamma_{\ell\nu}\cos\theta, \tag{1}$$

where $\gamma_{s\nu}$ and $\gamma_{\ell\nu}$ are the solid and liquid surface energy, respectively; $\gamma_{s\ell}$ is the solid/liquid interfacial energy, and θ is the contact angle. The contact angle θ and the liquid surface energy $\gamma_{\ell\nu}$ are measurable parameters. In order to determine the surface energy of the solid through the measurement of the contact angle, various theoretical statements describing the interfacial energy $\gamma_{s\ell}$ as $\gamma_{s\ell}=f(\gamma_{\ell\nu},\gamma_{s\nu})$ were used. In this work, the harmonic-mean method was used:[18]

$$\gamma_{s\ell}=\gamma_{s\nu}+\gamma_{\ell\nu}-4\left(\frac{\gamma_{s\nu}^{d}\gamma_{\ell\nu}^{d}}{\gamma_{s\nu}^{d}+\gamma_{\ell\nu}^{d}}+\frac{\gamma_{s\nu}^{p}\gamma_{\ell\nu}^{p}}{\gamma_{s\nu}^{p}+\gamma_{\ell\nu}^{p}}\right). \tag{2}$$

From Eqs. (1) and (2), it can be derived:

$$(1+\cos\theta)\,\gamma_{\ell\nu}=4\left(\frac{\gamma_{s\nu}^{d}\gamma_{\ell\nu}^{d}}{\gamma_{s\nu}^{d}+\gamma_{\ell\nu}^{d}}+\frac{\gamma_{s\nu}^{p}\gamma_{\ell\nu}^{p}}{\gamma_{s\nu}^{p}+\gamma_{\ell\nu}^{p}}\right). \tag{3}$$

Here, $\gamma_{\ell\nu}=\gamma_{\ell\nu}^{d}+\gamma_{\ell\nu}^{p}$ and the superscripts d and p refer to the dispersion and polar components. When two liquids are used, and the values of $\gamma_{\ell\nu}^{d}$ and $\gamma_{\ell\nu}^{p}$ for these liquids are known, the dispersive and polar components of the solid surface energy ($\gamma_{s\nu}^{d}$ and $\gamma_{s\nu}^{p}$) can be obtained by solving the two simultaneous equations.

The measurement of the contact angle of unimplanted and implanted UHMWPE were carried out in atmospheric conditions at a temperature of 20 °C using a VCA Optima device from AST Products, Inc. The test liquids (water and formamide), along with their surface energy ($\gamma_{\ell\nu}$) as well as the dispersive ($\gamma_{\ell\nu}^{d}$) and polar ($\gamma_{\ell\nu}^{p}$) components, are detailed in Table I. A droplet with the volume of 2 μl was released onto the surface of samples from a syringe needle. The contour of the liquid drop on the solid surface was captured by a charge coupled device camera after 10 s, which was to guarantee that the liquid drops had reached equilibrium. For each sample and liquid, at least six drops were measured.

C. Raman and morphological analysis

A micro-Raman spectroscopy (Raman scope, Renishaw 1000) with 514.5 nm Ar^{+} laser light was used to characterize the structural nature of the samples. The laser output power was 10 mW and 50% of laser power was filtered in order to reduce the power density on the samples. The morphology and roughness of unimplanted and implanted UHMWPE were analyzed by AFM and surface profiler (Tencor P-10).

III. RESULTS AND DISCUSSIONS

Figure 1 shows the measured contact angle for UHMWPE implanted with N_2^{+} and $C_3H_8^{+}$ ions implantation at various fluences and liquids. It can be very clearly noted that the contact angle vastly decreases after ion implantation regardless of ion species, fluences, and test liquids. The variation of the contact angle with the fluences for water shows the same tendency as formamide. For the N_2^{+} implanted samples, as the fluence increases the contact angle decreases [Fig. 1(a)]. This is consistent with Brun *et al.*'s results.[19] They reported the modification of a copolymer of polyethylene–polypropylene by alpha ionizing radiation, and found that the contact angle for water decreased from 92° to 76° by increasing the fluence from 10^{11} to 10^{15} ions/cm^2. However, it is worth noting that the contact angle of UHMWPE implanted with $C_3H_8^{+}$ at various fluences (1×10^{14} to 5×10^{15} ions/cm^2) reveals an inverse tendency as compared to that of N_2^{+} implantation. The contact angle decreases after $C_3H_8^{+}$ implantation, and then begins to increase with increases of the fluence [Fig. 1(b)].

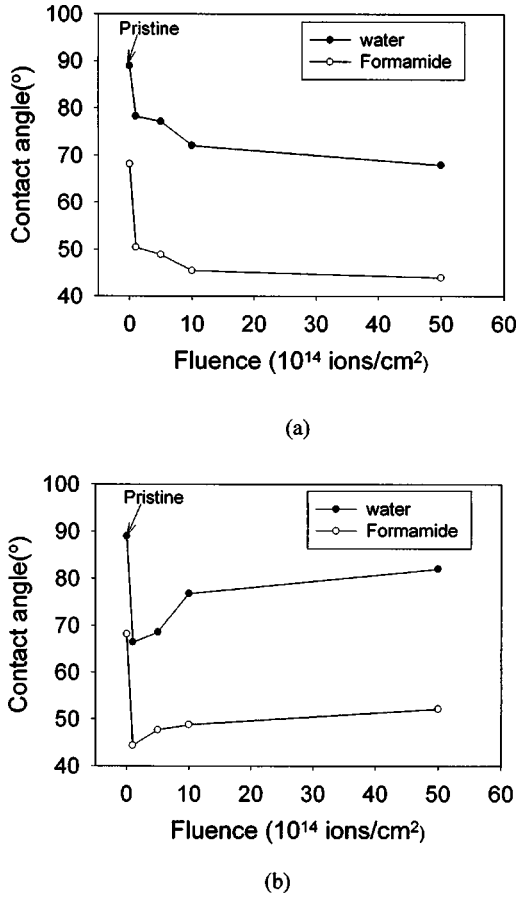

FIG. 1. Contact angle of ion implanted UHMWPE as a function of fluence: (a) N_2^{+} ion implantation and (b) $C_3H_8^{+}$ ion implantation.

The dispersive and polar components and total surface energy of unimplanted and implanted UHMWPE are calculated according to Eq. (3) and shown in Fig. 2. Compared to the pristine, the total surface energy increases significantly after implanting with the fluence of 1×10^{14} ions/cm^2 regardless of ion species, then the total surface energy slightly increases for N_2^{+} implanted UHMWPE and decreases slightly for $C_3H_8^{+}$ implanted UHMWPE with the further increase of fluence. Moreover, it is found that the significant increase in the total surface energy for N_2^{+} implantation at

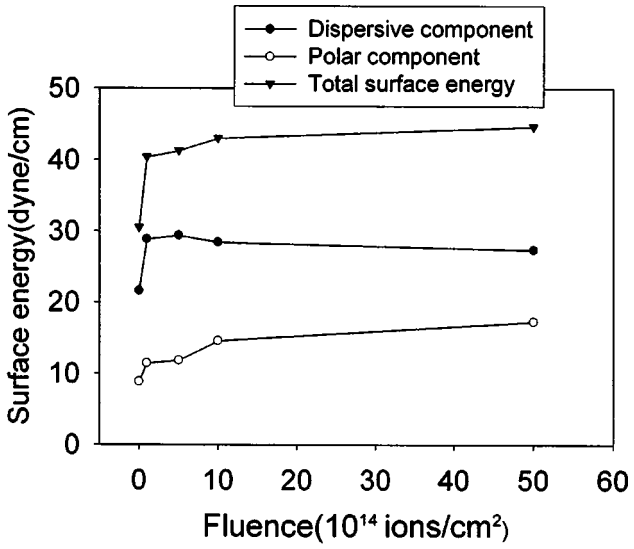

(a)

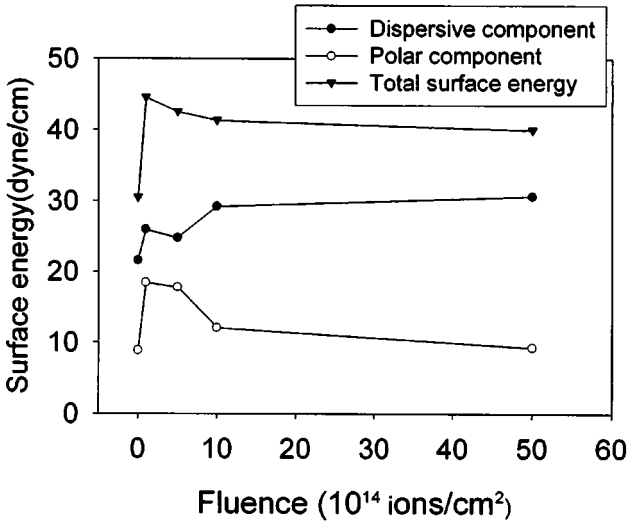

(b)

FIG. 2. Dispersive and polar components and total surface energy of ion implanted UHMWPE as a function of fluence: (a) N_2^+ ion implantation and (b) $C_3H_8^+$ ion implantation.

the fluence of 1×10^{14} ions/cm^2 compared to the pristine is mainly due to the increase of the dispersive component, and the slight increase of the total surface energy with the further increase of the fluence is ascribed to the increase of the polar component, the dispersive component keeps almost constant. Whereas, the contribution of the polar component to the total surface energy for $C_3H_8^+$ implanted UHMWPE with the fluence of 1×10^{14} ions/cm^2 is more than the dispersive component. The dispersive component at the fluence of 1×10^{15} ions/cm^2 is increased and equivalent to that of N_2^+ implantation at the fluence of 1×10^{14} ions/cm^2. The decrease of the total surface energy with the further increase of the fluence is attributed to the decrease of the polar component.

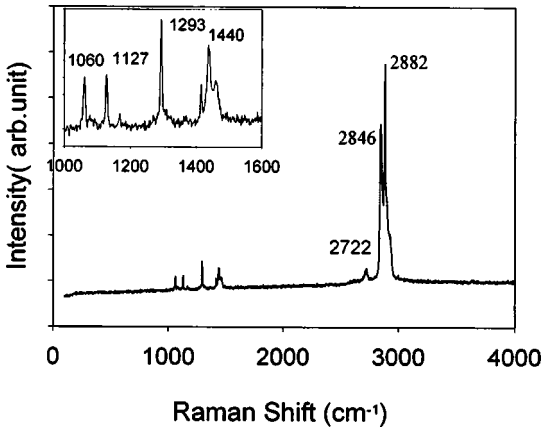

FIG. 3. Raman spectrum of the pristine UHMWPE sample.

Raman spectrum was used to characterize the structural change before and after implantation. For the pristine sample, several sharp peaks at 1060, 1127, 1293, 1440, 2722, 2846, and 2882 cm^{-1} can be observed (Fig. 3). The bands at 1060 and 1127 cm^{-1} with weak intensity are from the C—C skeletal stretching. The band at 1293 cm^{-1} with medium intensity is —CH_2— in-phase twisting mode and the band at 1440 cm^{-1} originates from the —CH_2— deformation stretching. The bands at 2846 and 2882 cm^{-1} with strong intensity can be attributed to the symmetric and asymmetric CH_2 stretchings.[20] Usually, the band at 2722 cm^{-1} cannot be observed in the Raman spectrum of polyethylene $[—CH_2—]_n$. The band may be ascribed to the —CH(=O) stretching caused by oxygen contamination on the surface.[20] Raman spectra of N_2^+ implanted UHMWPE with different fluences are shown in Fig. 4. After N_2^+ implantation with the fluence of 1×10^{14} ions/cm^2, it is observed that the effect of the fluorescence on the Raman spectrum is enhanced [Fig. 4(a)]. This can be ascribed to the increase of the defects in the polyethylene crystal caused by the implantation of energetic particles. The relative intensities of the bands at 1060, 1127, 1293, 1440, 2722, 2846, and 2882 cm^{-1} are all decreased, which suggests that the chemical structure of the UHMWPE has changed after implantation. Specifically, the relative intensity of the band at 1293 cm^{-1} increases with the n value of the $[—CH_2—]_n$. So the decrease of the relative intensity of the band at 1293 in our spectrum indicates that the chain of UHMWPE is broken and the length of the chain becomes much smaller than that of unimplanted UHMWPE.[20] By increasing the fluence (5×10^{14} ions/cm^2), the bands at 1060, 1127, 1293, and 1440 cm^{-1} disappear [Fig. 4(b)]. When the fluence is above 1×10^{15} ions/cm^2, a broadband around 1560 cm^{-1} appears [Figs. 4(c) and 4(d)] which can be ascribed to the hydrogenated amorphous carbon phase.[21] Raman spectra of $C_3H_8^+$ implanted UHMWPE with different fluences reveal very similar changes to N_2^+ implanted UHMWPE, as illustrated in Fig. 5. These broadbands around 1560 cm^{-1} are fitted by Lorentzian and Gaussian shapes and the fitting results including the D (disorder) and G (graphite) peak positions and the ratio of their intensity (I_D/I_G) are shown in Table II. It is found that for the N_2^+ implantation the D and G peaks shift to

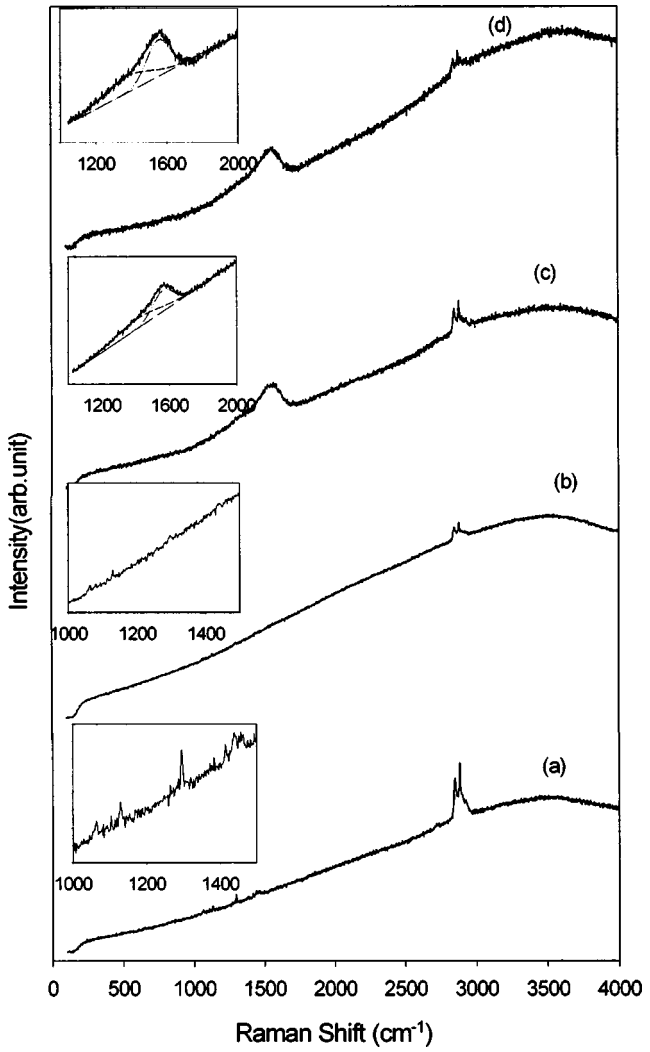

FIG. 4. Raman spectra of UHMWPE implanted with N_2^+ at different fluences: (a) 1×10^{14} ions/cm^2, (b) 5×10^{14} ions/cm^2, (c) 1×10^{15} ions/cm^2, and (d) 5×10^{15} ions/cm^2.

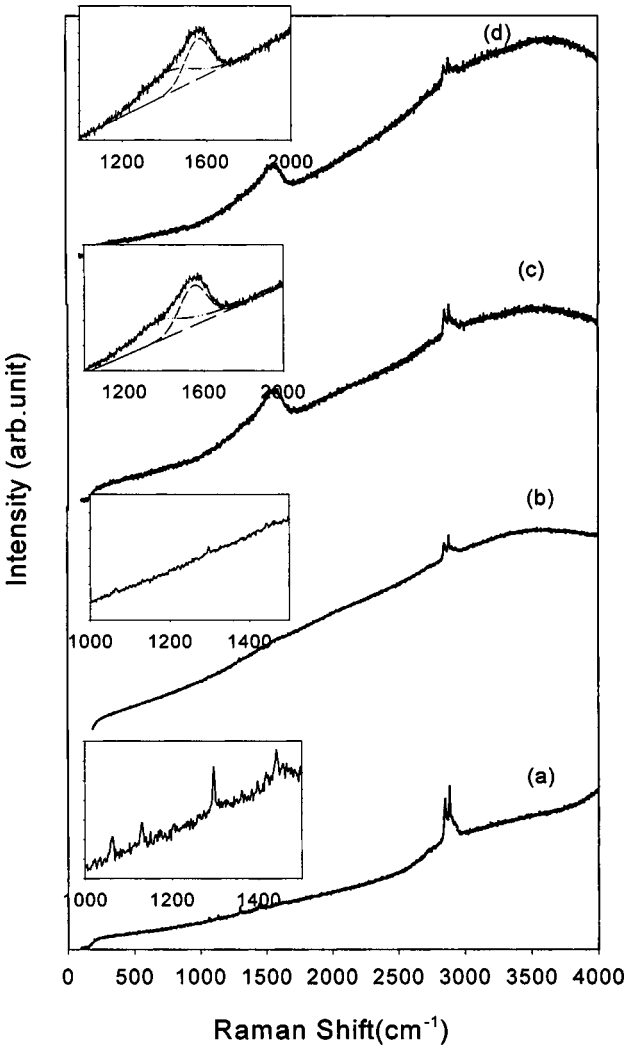

FIG. 5. Raman spectra of UHMWPE implanted with $C_3H_8^+$ at different fluences: (a) 1×10^{14} ions/cm^2, (b) 5×10^{14} ions/cm^2, (c) 1×10^{15} ions/cm^2, and (d) 5×10^{15} ions/cm^2.

a lower frequency and I_D/I_G decreases when the fluence increases from 1×10^{15} ions/cm^2 to 5×10^{15} ions/cm^2, whereas for the $C_3H_8^+$ implantation, the *D* and *G* peaks shift to a higher frequency and I_D/I_G increases when the fluence increases from 1×10^{15} ions/cm^2 to 5×10^{15} ions/cm^2. The simultaneous downshift in both *G* and *D* peaks are indicative of the increasing of the number of sp^3-bonded atomic sites,[22,23] and I_D/I_G varies inversely with the crystal size of graphite.[24] Consequently, the modified layer for N_2^+ implantation at the fluence of 5×10^{15} ions/cm^2 is more diamondlike carbon than that at 1×10^{15} ions/cm^2 and $C_3H_8^+$ implantation is inverse. In addition, the modified layer for $C_3H_8^+$ implantation is more polymerlike than for N_2^+ implantation.

According to Neumann,[25] the influence of surface roughness on the contact angle can be expressed as: The smoother the contact surface, the smaller the contact angle. So, in order to estimate the effect of surface roughness on surface energy, the surface morphology and roughness of unimplanted and implanted UHMWPE were characterized by AFM and a surface profiler. Figure 6 shows the AFM images of UHMWPE unimplanted and N_2^+ implanted with the fluence of 5×10^{14} ions/cm^2. It is observed that after implantation there are many irregularities on the surface and, hence, roughness increases. The surface roughness of N_2^+ and $C_3H_8^+$ implanted UHMWPE versus the fluence is illustrated in Fig. 7. The surface roughness increases with the increase of the fluence regardless of ion implantation species. Compared with N_2^+ implantation, the samples implanted by $C_3H_8^+$ reveal small roughness. These may be attributed to the higher average energy of each atom for N_2^+ implantation (N; 40 keV, C; 22 keV).

TABLE II. Fitting results of Raman spectra.

	G peak (cm^{-1})	*D* peak (cm^{-1})	I_D/I_G
N_2^+ (1×10^{15} ions/cm^2)	1563	1413	0.46
N_2^+ (5×10^{15} ions/cm^2)	1552	1395	0.44
$C_3H_8^+$ (1×10^{15} ions/cm^2)	1554	1411	0.55
$C_3H_8^+$ (5×10^{15} ions/cm^2)	1560	1426	0.60

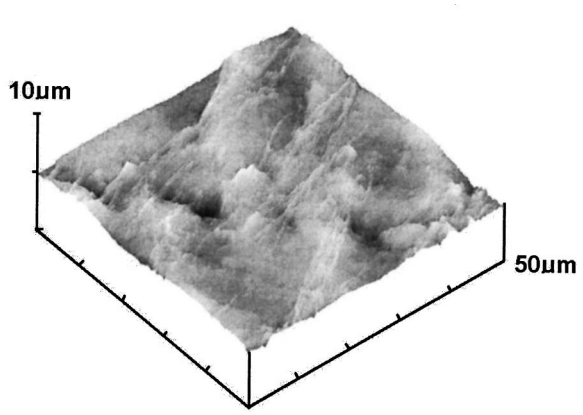

(a)

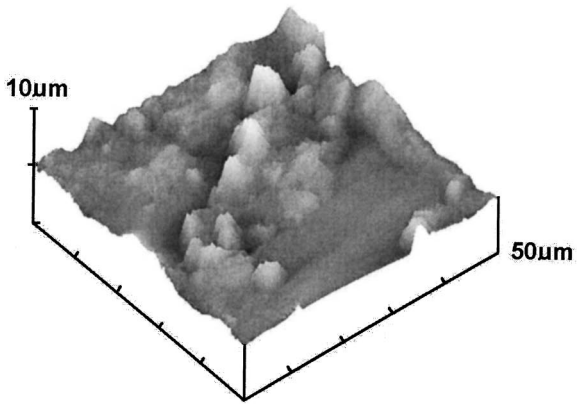

(b)

FIG. 6. AFM images of UHMWPE: (a) pristine and (b) N_2^+ implantation with a fluence of 5×10^{14} ions/cm^2.

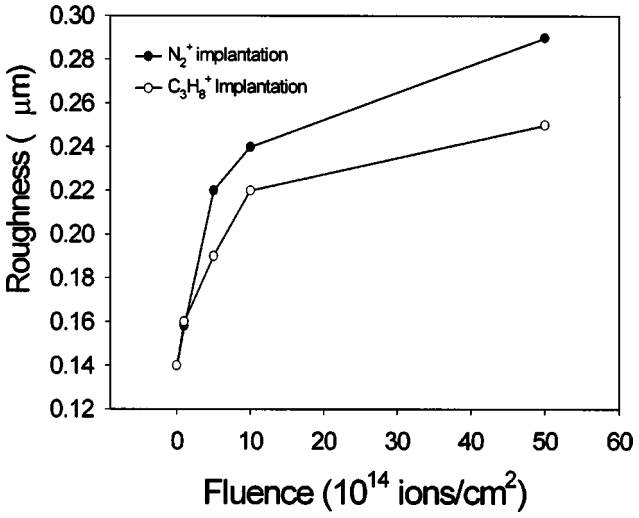

FIG. 7. Roughness of ion implanted UHMWPE as a function of fluence.

From these results, it is found that the changes of Raman spectra and roughness with the fluences after different ion implantation species are very similar. However, the surface energy of N_2^+ and $C_3H_8^+$ implanted UHMWPE with a different fluence reveals the reverse changes except the increase of the surface energy compared to the unimplanted samples. UHMWPE is a kind of low-surface-energy polymer, which is ascribed to its flexible linear saturation chain structure. The surface energy arises from an imbalance of forces acting on molecules or atoms at the surface relative to those in the bulk. After implantation, the breakage of the chain and formation of the cross linking lead to the enhancement of the interaction of different molecular chain and, hence, the initial increase of the surface energy. In addition, dehydrogenation caused by ion implantation may lead to the formation of the unsaturated bonds and, hence, increase the polar component. The increase of the surface energy of N_2^+ implanted UHMWPE with the increasing fluence can be attributed to the increase of the polar component caused by the formation of more C—N bonds and unsaturated C—H bonds.[14] Whereas for $C_3H_8^+$ implantation, the decrease of the surface energy may be due to a more saturated chemical group such as CH_3 (hydrophobic group) on the surface and the decrease of the polar component. Nakao *et al.*[26] showed that some carbon free radicals caused by ion implantation could recombine with atmospheric oxygen, and surface energy is sensitive to the surface property of materials. So, chemical and physical absorption are also very important factors for affecting the surface energy. These need further investigation. Associated with the evolution of surface roughness and the contact angle, i.e., surface energy with an increase of the fluence, a direct relationship cannot be obtained between the surface roughness and surface energy. Consequently, the chemical modification of the surface plays a more important role in the surface change than the surface roughness.

IV. CONCLUSIONS

The effect of ion implantation including ion species and the fluences on the surface energy of UHMWPE has been investigated. The total surface energy increases significantly after implanting with the fluence of 1×10^{14} ions/cm^2 regardless of ion species, then, the total surface energy slightly increases for N_2^+ implanted UHMWPE and decreases slightly for $C_3H_8^+$ implanted UHMWPE with a further increase of fluence.

The structural changes of UHMWPE with a different fluence for different ion species are very similar. After implantation, the linear chains of UHMWPE are damaged and cross linking is generated. As the fluence increases, the modified layer becomes more disordered, and when the fluence exceeds 1×10^{15} ions/cm^2, the surface becomes amorphous hydrogenated carbon. The surface roughness increases with an increase in the fluence regardless of ion implantation species.

The breakage of the chain and formation of the cross linking lead to the enhancement of the interaction of different molecular chains, hence, the increase of surface energy. In addition, dehydrogenation caused by ion implantation may lead to the formation of unsaturated bonds, hence, an increase of the polar component. The introduction of polar bonds (C—N) for N_2^+ implantation and hydrophobic groups,

such as CH_3 for $C_3H_8^+$ implantation, may be responsible for their different surface changes with the fluence.

[1] J. S. Williams, Rep. Prog. Phys. **49**, 491 (1986).
[2] G. Terwagne, S. Lucas, and F. Bodart, Nucl. Instrum. Methods Phys. Res. B **59**, 93 (1990).
[3] E. Wieser, R. Grötzschel, A. Mücklich, and F. Prokert, Nucl. Instrum. Methods Phys. Res. B **134**, 365 (1998).
[4] M. Fujinami, R. Suzuki, T. Ohdaira, and T. Mikado, Appl. Surf. Sci. **149**, 188 (1999).
[5] G. Marletta, Nucl. Instrum. Methods Phys. Res. B **46**, 295 (1990).
[6] J. C. Pivin, Nucl. Instrum. Methods Phys. Res. B **84**, 484 (1994).
[7] E. H. Lee, G. R. Rao, M. B. Lewis, and C. K. Mamsur, J. Mater. Res. **9**, 1043 (1994).
[8] H. Tsuji, H. Satoh, S. Ikeda, Y. Gotoh, and J. Ishikawa, Nucl. Instrum. Methods Phys. Res. B **141**, 197 (1998).
[9] H. Tsuji, H. Satoh, S. Ikeda, Y. Gotoh, and J. Ishikawa, Surf. Coat. Technol. **103**, 1124 (1998).
[10] Y. Suzuki, M. Kusakabe, K. Kusakable, H. Akiba, and M. Iwaki, Nucl. Instrum. Methods Phys. Res. B **59**, 698 (1991).
[11] Y. Oshida, R. Sachdeva, S. Miyazaki, and J. Daly, J. Mater. Sci.: Mater. Med. **4**, 443 (1993).
[12] S. B. Goodman, R. C. Chin, S. S. Chiou, D. J. Schurman, S. T. Woolson, and M. P. Masada, Clin. Orthop. **224**, 182 (1989).
[13] A. V. Lombardi, Jr., T. H. Mallory, B. K. Vaughn, and P. Drouillard, J. Bone. Joint Surg. A **71**, 1337 (1989).
[14] J. S. Chen *et al.* Nucl. Instrum. Methods Phys. Res. B **169**, 26 (2000).
[15] C. Allen, A. Bloyce, and T. Bell, Tribol. Int. **29**, 527 (1996).
[16] H. Dong and T. Bell, Surf. Coat. Technol. **111**, 29 (1999).
[17] T. Young, Philos. Trans. R. Soc. London **9**, 255 (1805).
[18] S. Wu, *Polymer Interface and Adhesion* (Marcel Dekker, New York, 1982), pp. 178–181.
[19] C. Brun, A. Chambaudet, C. Mavon, F. Berger, M. Fromm, and F. Jaffiol, Appl. Surf. Sci. **157**, 85 (2000).
[20] D. Lin-Vien, N. B. Colthup, W. G. Fateley, and J. G. Grasselli, *The Handbook of Infrared and Raman Characteristics Frequencies of Organic Molecules* (Academic, New York, 1991).
[21] J. C. Pivin, Thin Solid Films **263**, 185 (1995).
[22] R. O. Dillon, A. Woollam, and V. Katkanant, Phys. Rev. B **29**, 3482 (1984).
[23] M. A. Tamor, J. A. Haire, C. H. Wu, and K. C. Hass, Appl. Phys. Lett. **54**, 123 (1989).
[24] F. Tuinstra and J. L. Koenig, J. Chem. Phys. **53**, 1126 (1970).
[25] A. W. Neumann, Adv. Colloid Interface Sci. **4**, 438 (1974).
[26] A. Nokao, Y. Suzuki, M. Kaibara, T. Tsukamoto, and M. Ivaki, J. Electron Spectrosc. Relat. Phenom. **88**, 945 (1998).